https://doi.org/10.5194/egusphere-2024-451
Preprint. Discussion started: 28 February 2024

Signatures of Ocean Oxygen-Depleted Waters along the Sumatra-Java Coasts in the Southeastern Tropical Indian Ocean

Faisal Hamzah[1†], Iis Triyulianti[2†], Agus Setiawan[2], Intan S. Nurhati[2], Bayu Priyono[1], Dessy Berlianty[1], Muhammad Fadli[2], Rafidha Dh Ahmad Opier[2], Teguh Agustiadi[1], Marsya J. Rugebregt[2], Weidong Yu[3], Zexun Wei[4,5], Huiwu Wang[4,5], Raden D. Susanto[6], and Priyadi D. Santoso[2]

[1]Research Center for Oceanography, National Research and Innovation Agency (BRIN), Jakarta 14430, Indonesia.
[2]Research Center for Deep Sea, National Research and Innovation Agency (BRIN), Jakarta 14430, Indonesia
[3]School of Atmospheric Sciences, Sun Yat-Sen University, Zhuhai, China.
[4]First Institute of Oceanography, Ministry of Natural Resources, Qingdao, China.
[5]Laboratory for Regional Oceanography and Numerical Modeling, Pilot National Laboratory for Marine Science and Technology, Qingdao, China.
[6]Department of Atmospheric and Oceanic Science, University of Maryland, College Park, MD 20742, USA.
[†] These authors contributed equally to this work and shared first authorship.

Correspondence to: Faisal Hamzah (faisal.hamzah@brin.go.id) and Iis Triyulianti (iis.triyulianti@brin.go.id).

https://doi.org/10.5194/egusphere-2024-451
Preprint. Discussion started: 28 February 2024

Abstract. A prominent ocean region exhibiting depleted oxygen concentration is the northern Indian Ocean, whose projected deoxygenation trend in response to climate change requires a comprehensive understanding of the roles of ocean dynamics. We present newly compiled *in situ* data across platforms (e.g. cruises, Argo, buoy) in the Indonesian coasts of Sumatra and Java between 2010-2022. Combined with reanalysis products, our data detect oxygen-depleted waters attributed to the eastward advection of the northern Indian Ocean waters and monsoon-driven coastal upwelling. Oxygen limited zones (OLZs, DO < 60 μmol kg^{-1}) occupy various depths off the Sumatra-Java coasts, in which dissolved oxygen (DO) reaches ~40 μmol kg^{-1} in northwest Sumatra. The eastward propagating Equatorial Counter Current plays a major role in delivering the oxygen-depleted waters during the boreal summer; similarly, the South Equatorial Counter Current in the winter monsoon and the Wyrtki Jet during the transition months. Coastal upwelling regulates DO variations via primary production and the respiration of organic matter at intermediate depths in southern Java as the upwelled waters being advected westward towards Sumatra in the summer monsoon. Indonesian Throughflow with enriched organic matter modifies the oxygenated-depleted waters at its outlets. We observe a trend towards deepened OLZ in western Sumatra, while positive Indian Ocean Dipole events (2006, 2012, 2015, 2019) lower DO in the thermocline depths of southern Java on the interannual timescale. Altogether, high-resolution observational biogeochemical data are key to advance our understanding of dynamical DO changes in the southeastern tropical Indian Ocean under the global deoxygenation trend.

Keywords: Deoxygenation, oxygen limited zone, upwelling, Indonesia, southeastern tropical Indian Ocean

https://doi.org/10.5194/egusphere-2024-451
Preprint. Discussion started: 28 February 2024

Short Summary

We provide new insights on the presence of oxygen-depleted waters along the Indonesian coasts of Sumatra and Java attributed to the eastward advection of the northern Indian Ocean waters and monsoon-driven upwelling. Combined in situ and reanalysis data elucidate the complex interplay of oceanographic processes responsible for the observed oxygen in the region. The knowledge is crucial for research and management strategies to mitigate deoxygenation impacts on marine ecosystems in Indonesia.

https://doi.org/10.5194/egusphere-2024-451
Preprint. Discussion started: 28 February 2024

1 Introduction

As human activities alter the ocean globally, deoxygenation in the open ocean and coastal systems has emerged as one of the most evident responses to climate change (Breitburg et al., 2018; Bindoff et al., 2019). Global coverage of deoxygenation varies spatially with the presence of oxygen minimum zones (OMZs) in the northern Indian Ocean and the eastern boundaries of the Pacific and Atlantic Oceans (Karstensen et al., 2008; Paulmier and Ruiz-Pino, 2009; Keeling et al., 2010; Breitburg et al., 2018). The global ocean has lost an estimated 2% (4.8 ± 2.1 Pmoles) of oxygen, showing marked changes in the upper 1,000 m section since the 1980s (Diaz and Rosenberg, 2008; Ito et al., 2017; Schmidtko et al., 2017). Ocean deoxygenation is expanding in a warmer climate, with recent CMIP6 Earth system models suggesting greater deoxygenation trends than previous model ensembles (Canadell et al., 2021 and references therein). At regional scales, enhanced nutrients via ocean upwelling and coastal eutrophication leading to excessive respiratory oxygen demand may exacerbate the global deoxygenation trend (Oschlies et al., 2008; Gilbert et al., 2010; Pitcher et al., 2021). Since the mid-20th century, at least 400 coastal areas have become hypoxic, a condition in which seawater DO concentration reaches less than 63 μmol $l^{-1} \approx 2$ mg l^{-1} or approximately 30% oxygen saturation, with varying nonlinear perturbations on marine organisms (Diaz and Rosenberg, 2008; Vaquer-Sunyer et al., 2008).

Weakened ocean ventilation in a warmer climate primarily drives global deoxygenation in addition to the reduced solubility of seawater DO, which highlights the critical role of ocean dynamics. Reduced oxygen ventilation into the ocean interior due to more stratified oceans accounts for ~85% of the global deoxygenation trend (Helm et al., 2011; Schmidtko et al., 2017; Breitburg et al., 2018; Bindoff et al., 2019; Canadell et al., 2021). Seawater oxygen concentration is relatively higher in the upper ocean with air-sea flux and photosynthetic activities, while it diminishes with the oxygen-consuming biogeochemical processes (e.g. the decomposition of organic matters, remineralization) in the water column and bottom sediment (Oschlies et al., 2008; Pitcher et al., 2021). Oxygen-deficient conditions arise when oxygen consumption rates exceed renewal via ventilation or mid-depth injections of oxygenated waters (Wyrtki, 1962; Hamme and Keeling, 2008).

A significant portion of the global ocean OMZs occurs in the Arabian Sea and the Bay of Bengal (BoB), owing to the weak ventilation and high oxygen consumption at intermediate depths driven by high productivity and lithogenic inputs in the Arabian Sea and the BoB, respectively (Helly and Levin, 2004; Paulmier and Ruiz-Pino, 2009; Rixen et al., 2020; Shenoy et al., 2020; Pitcher et al., 2021). Unlike in the Pacific and the Atlantic Oceans, low oxygen conditions do not develop along the eastern

https://doi.org/10.5194/egusphere-2024-451
Preprint. Discussion started: 28 February 2024

boundary but are evident in the northern Indian Ocean. The area is distinctly characterized by the low-latitude continental boundary that restricts the formation of subsurface water masses. Ocean ventilation in the basin is influenced by the more oxygenated Indian Central Water (ICW) and the fresh and high silicate Indonesian throughflow (ITF) outflow (often referred to as the Australasian Mediterranean Water or the Banda Sea Water), with a minor contribution of the warm and saline Red Sea and the Persian Gulf Waters (You and Tomzak, 1992; Talley and Sprintall, 2005). The ICW, formed in the subtropical southern Indian Ocean, crosses the equator near the western boundary primarily during the southwest monsoon in the Arabian Sea (Swallow, 1984; Naqvi et al., 2010). In the BoB, high freshwater influx leads to a strong salinity stratification that hinders ventilation (You and Tomzak, 1992). Vertical eddy mixing contributes to oxygen ventilation in the Arabian Sea and the BoB (McCreary et al., 2013; Sarma and Bhaskar, 2020). The Arabian Sea experiences a perennial high productivity due to upwelling during the southwest monsoon in boreal summer and convective overturning during the winter (Naqvi et al., 2006). While primary productivity is relatively lower in the BoB, the ballast effect of lithogenic inputs enhances the downward export of organic matter in the basin (Rao et al., 1994; Al Azhar et al., 2017).

In this study, we present the dynamics of oxygen-depleted waters along the Indonesian coasts of Sumatra and Java in the southeast tropical Indian Ocean (SETIO) using DO time series obtained from international cruise campaigns between 2010-2022, complemented by available Argo float, buoy and reanalysis products. Complex ocean circulations in the Indian Ocean advect the oxygen-depleted OMZ waters, thus potentially affecting marine ecosystems. Coastal currents in the northern Indian Ocean propagate eastward during the summer, and the Arabian Sea waters flow towards the Sumatra coast during the winter via the Equatorial Counter Current or ECC (Rahaman et al., 2020; Phillips et al., 2021). The eastward Wyrtki Jet at the upper 100 m of the equatorial Indian Ocean is most intense during the intermonsoon in May and November, reaching 18.74 and 16.83 Sv, respectively (Wyrtki, 1973; McPhaden et al., 2015). The eastward Equatorial Under Current (EUC) at around 90-170 m depths is strongest in April and October (Iskandar et al., 2009). Knowledge gaps remain on the characteristics of oxygen-depleted waters of the study area and their associated mechanisms, such as the influences of seasonal upwelling and the Indo-Pacific climate variability.

2 Materials and Methods

2.1 Study area

https://doi.org/10.5194/egusphere-2024-451
Preprint. Discussion started: 28 February 2024

The biogeochemistry of the Sumatra-Java coasts is influenced by several factors including lateral currents, the ITF and monsoon-driven upwelling. These processes significantly affect nutrient distribution, primary productivity and oxygen levels in the region. The ITF is crucial in delivering nutrients, particularly in the upper 300-400 m, which subsequently influences oxygen consumption in the water column (Talley and Sprintall, 2005; Ayers et al., 2014). Seasonal upwelling along the Sumatra-Java coasts peaks in June-November during the southeast monsoon in the boreal summer associated with the Ekman transport and mesoscales eddies that generate high primary productivity (Susanto et al., 2006; Yang et al., 2019; Wirasatriya et al., 2020). Major currents in the region are important in distributing saline and oxygen-depleted waters from the western Indian Ocean and relatively fresher waters of the ITF. The semi-annually reversing South Java Current (SJC) and it's Under Current (SJUC) form the eastern boundary current system that flows along the coasts of Sumatra and Java (Sprintall et al., 1999, 2010; Wijffels et al., 2002). The SJC and SJUC contribute to exchanging freshwater and saltier waters in the SETIO. At deeper depths, the North Indian Intermediate Water (NIIW), characterized by high salinity and low oxygen, is transported eastward by the SJUC (Sprintall et al., 2010). The formation of the saltier NIIW is located in the northwestern Indian Ocean (You and Tomczak, 1993; Wijffels et al., 2002). The South Equatorial Current (SEC) also plays a significant role in the region, flowing westward around 12ºS and bringing fresher and warmer waters. The current connects directly with the Agulhas Current and is part of the global ocean current system through the Ocean Conveyor Belt (Reppin et al., 1999; Makarim et al., 2019). In addition, the Sumatra-Java coasts are strongly influenced by Indo-Pacific climate variability, such as the El Niño-Southern Oscillation (ENSO) and the Indian Ocean Dipole (IOD) phenomenon, which can further modulate the biogeochemical processes and ecosystem dynamics in the region.

2.2 Cruise-based observational data

The collected *in situ* temperature, salinity and DO data presented herein are the product of several international cruise campaigns conducted in 2011-2013, 2015-2016, 2018-2019 and 2022 (Fig. 1). The cruises comprise the Java Upwelling Variation Observation (JUVO) conducted in 2011, 2012, 2015 and 2016, the Monsoon Onset Monitoring, Its Social and Ecosystem Impacts (MOMSEI) in 2013, the Transport Indonesian seas, Upwelling and Mixing Physics (TRIUMPH) in 2018 and 2019, and the Ekspedisi Widya Nusantara (EWIN) in 2022 using the RV Baruna Jaya I, RV Baruna Jaya III, RV Baruna Jaya III and RV Madidihang 03 (Appendix Table A1). These cruises deployed shipboard and

https://doi.org/10.5194/egusphere-2024-451
Preprint. Discussion started: 28 February 2024

subsurface-moored conductivity-temperature-depth (CTD) and DO sensors at sampling stations, some repeated over multiple years.

Shipboard data were collected using Sea-Bird Electronic (SBE) 9Plus and 19Plus CTDs, equipped with an SBE 5T pump and an auxiliary SBE 43 DO sensor. The accuracies of the SBE 9Plus CTD were 0.0003 S m^{-1} (conductivity), 0.001°C (temperature), and 0.015% (depth) of the full-scale ranges. The SBE 19Plus CTD had measurement accuracies of 0.0005 S m^{-1} (conductivity), 0.005°C (temperature), and 0.02% (depth). The SBE 43 DO sensor had an accuracy of ± 2% of saturation. The deployment was conducted from the surface to the near bottom or maximum wire length, with sampling speeds of 24 Hz (9 Plus) and 4 Hz (19 Plus), and the casting speed was kept at 0.5 m s^{-1} to minimize the noise during measurement. The measured CTD data underwent quality control (QC) methods provided by the SBE data processing software (i.e. data conversion, wild edit, filtering, aligning CTD, cell thermal mass, loop edit, deriving variables based on EOS 80 standard, and bin average) with a final manual screening step to ensure the result of the QC process, following modified methods of Valcheva and Palazov (2010) and Sea-Bird Scientific (2017).

The moored CTD-DO sensors (SBE37 IMP-ODO) were deployed at 10 and 300 m depths with a 1-hour interval. CTD and DO measurements had accuracies of ± 0.0003 S m^{-1}, 0.002°C, 0.1% and 0.1% of the full-scale ranges, respectively. Each instrument followed a pre-deployment check including a comparison with the shipboard data. The data also followed QC methods (i.e. data conversion, wild edit, and deriving variables based on the EOS 80 standard).

2.3 Argo float and RAMA buoy data

Data from two Argo floats and a Research Moored Array for African - Asian - Australian Monsoon Analysis and Prediction (RAMA) buoy in the eastern Indian Ocean complement our cruise-based measurements. Two Argo floats provide temperature and salinity data across depths from the study area (ID #1901944 for 2010-2021 and #5905417 for 2016-2021). To establish a robust dataset, we use the adjusted QC flagged data (i.e. with real-time QC tests and adjusted values to account for statistical error estimates). The RAMA buoy (8ºS, 99.56ºE) equipped with CTD and DO sensors at 10 and 300 m depths provide continuous data from April 2014 to March 2015.

2.4 Cross-sectional annual and seasonal DO concentrations across depths

We assess annual, winter (Jan-Mar) and summer (July-Sept) climatology DO concentrations across depths and parallel cross-sections over the period 2000-2020 using the World Ocean Atlas 2018

https://doi.org/10.5194/egusphere-2024-451
Preprint. Discussion started: 28 February 2024

(WOA18) data (Garcia et al., 2019). The dataset is a product of shipboard and underway instruments, moored buoys and Argo float data with a 1° spatial resolution. The WOA18 annual climatology data is available across 0-5,500 m depths (102 standard depths) and 0-1,500 m (57 standard depths) for the seasonal and monthly climatology data. We define the coastal, transition and SEC cross-sections with increasing distances from Sumatra and Java Islands.

2.5 Reanalysis DO product and *in situ*-model validation

We assess reanalysis temperature, salinity, ocean currents and DO data of the Copernicus Marine Environment Monitoring Service (CMEMS) between 2000-2020 with the *in situ* data from three observational stations from our 2022 cruise to provide insights on long-term DO variability over the Indian Ocean. The CMEMS dataset is a hindcast global ocean data using the Pelagic Interactions Schemes for Carbon and Ecosystem Studies (PISCES) biogeochemical model of intermediate complexity (Aumont, 2015). The three stations used in the *in-situ* model validation are St.04 (104.39°E, 6.54°S), St.13 (106.91°E, 8.12°S) and St.14 (107.07°E, 7.71°S). In evaluating the model's performance, we calculate the relative root mean square error (RRMSE) and mean absolute percentage error (MAPE) to assess the difference between predicted and actual values, with values closer to zero indicating a better match. The accuracy of the model can be considered as very good when RRMSE<10%, good (10%<RRMSE<20%), reasonable (20%<RRMSE<30%) or poor (RRMSE> 30%) (Li et al., 2013). Similar classifications are applied to the MAPE except for the poor (MAPE>50%) category (Moreno et al., 2013). The calculated data show that RRMSE and MAPE are classified as good at St. 04 and very good at St. 13 and St. 14 (Appendix Table A2). The comparison between the modeled and observed DO shows biases, however, statistical analyses demonstrate a high agreement between the two datasets (Appendix Fig. A1). The reanalysis products underestimate DO concentrations at St. 04 and St.14, particularly around 100-700 m depths, while under and overestimate *in situ* data at St. 13 at the similar depths.

2.6 Identifying the presence of oxygen-depleted Arabian Sea water

In order to trace the eastward intrusion of the saline oxygen-depleted Arabian Sea water into our study area, we apply the assumption of water mass with salinity reaching 35 practical salinity scale (PSS). The assumption relies on the fact that subsurface water masses in the Sumatra-Java coast do not have such saline value, including the ITF outflow with ~34.6 PSS (Gordon et al., 1997; Makarim et

https://doi.org/10.5194/egusphere-2024-451
Preprint. Discussion started: 28 February 2024

al., 2019). Herein, the critical concentration delimiting OMZ is defined at 22 µmol kg^{-1}, and the OLZ at <60 µmol kg^{-1} following Espinosa-Diaz et al. (2021).

3 Results

3.1 Physical and biogeochemical characteristics of the water masses

Our cruise-based observational measurements reveal a warm and fresh water mass overlying more saline water masses in the Sumatra-Java coasts of the SETIO (Fig. 2). A buoyant, warm and low salinity (<33 PSS) water mass along the potential density (σ_θ) of 20-22 is prominent in the 2011, 2012, 2015 and 2022 data. Beneath this surface mixed layer, we observe a ~35 PSS salinity water mass along the σ_θ23-24 in 2011, 2012 and 2015, and along the σ_θ23-27 in 2019 and 2022. In 2016, a relatively more saline (35-36 PSS) water mass appear along the σ_θ24-27. High-salinity waters are also present at deeper depths along the σ_θ24.5 and σ_θ25-26 in 2019 and 2022. Most high-salinity waters are evident at stations southwest of the Sunda Strait.

Warm and fresh waters with relatively higher oxygen concentrations (164-197 µmol kg^{-1}) corroborate enhanced seawater DO from photosynthetic activities in the surface layer. High DO waters are present in the 32-34 PSS salinity ranges (Fig. 2b). The relationship between potential temperature and DO (θ-DO) hints at high oxygen concentrations in warmer ~29-30°C waters (Fig. 2c). Furthermore, DO concentrations with 34-35 PSS salinity decrease to 120 µmol kg^{-1} with concentrations that vary from one year to another. In the 2016 cruise data, we observe a DO concentration of ~167 µmol kg^{-1} with 33-36.3 PSS salinity, slightly different from those observed in 2011, 2012, 2015 and 2022. Similarly, DO data in 2019 show slightly erratic profiles along the potential temperature and salinity gradients. At deeper depth with ~35 PSS salinity, the DO concentration reaches 50 µmol kg^{-1}.

3.2 Cross-sectional oxygen distributions along the Sumatra-Java coasts

The WOA18 dataset, which serve to elucidate the influence of regional oceanography to seawater DO in our study site, show OLZs in the intermediate 200-1,000 m depths of the coastal section and in greater depths (500–1,000 m) of the transition section (Fig. 3). Overall, high DO (>180 mol kg^{-1}) characterizes the upper 100 m section of the Sumatra-Java coasts year-round. The OLZ tongue with ~35 PSS salinity extends eastward for about 1,000 km in the coastal section and 500 km in the transition section.

https://doi.org/10.5194/egusphere-2024-451
Preprint. Discussion started: 28 February 2024

The oxygen-depleted condition is absent in the SEC section, with DO<100 μmol kg^{-1} occupying between 700-1,200 m in the depth profiles. We find no trace of the inferred Arabian Sea water in the SEC section throughout the year.

Comparison of OLZ between seasons reveals a sharper eastward protruding pattern during the boreal summer that may be shaped by the presence of upper and below ocean currents advecting relatively more oxygenated water masses. The feature, centered around 700 m depth, may be related to more oxygenated water masses advected from the eastern Indian Ocean (see Fig. 4-Right).

Taken together, our analysis of the WOA18 DO dataset in the SETIO shows the imprint of eastward advected oxygen-depleted water mass from the northern Indian Ocean, with the roles of local ocean currents inhibiting its eastward propagation.

3.3 Horizontal depth profiles of oxygen in the Indian Ocean

The cross-sectional oxygen distribution may infer the influence of the oxygen-depleted northern Indian Ocean waters in the SETIO. The annual climatology DO between 100 and 1,000 m is shown in Figure 4-Left. At a shallower 100 m depth, DO of 60 μmol kg^{-1} (OLZ; black line) is evident in coastal regions of the western and eastern Arabian Sea and the BoB. At deeper depths, OLZ in the northern Indian Ocean covers a more extensive section and expands southward towards the equator. At around 200-600 m depths, the lowest DO concentration of ~40 μmol kg^{-1} is evident in the northwest of Sumatra westward of the 94°E longitude, consistent with the signature of the oxygen-depleted BoB water. While OMZ does not present at a 100 depth, it is evident in deeper depths, occupying the northern Arabian Sea and BoB around 200-400 m depths and most notably in the north of Arabian Sea at deeper >700 m depths, therefore lending support to the role of ocean dynamics in advecting oxygen-depleted water masses at those depths.

The spreading of the oxygen-depleted water at different depth levels is seasonally distinct. In the boreal winter, the OLZ is observed at 100 m depth along the coasts of the Arabian Sea and the western BoB that may be due to the West Indian Coastal Current (WICC), while the OMZ is only visible on the northern coast of BoB (Figure 4-Center). Low DO concentrations are also found in the center of the Arabian Sea. At 200-1000 m depths, the OLZ extends meridionally from the coast of Somalia in the western Indian Ocean to the Sumatra-Java coasts reaching the equator. The OMZ dominates the coastal area of the Arabian Sea and the southern BoB at ~200 m. Only at greater depths in the south of the Arabian Sea is the OMZ visible. During the boreal summer, the spreading of the

https://doi.org/10.5194/egusphere-2024-451
Preprint. Discussion started: 28 February 2024

oxygen-depleted water at deeper depth is similar to the winter, except in the upper 100 m with an apparent influence of continental margin (Fig. 4-Right).

OLZ and OMZ in the northern Indian Ocean expand southward, even crossing the equator as the depth increased. In the western Indian Ocean, OLZ reaches the 200 m depth at ~12ºN and the equator at 1000 m. This pattern is also evident in the eastern Indian Ocean, which may be caused by an eastward advection of low deoxygenated water due to a combination of the Summer Monsoon Current and the prolonged eastward WICC. While the southward extent of the OLZ in western Sumatra is similar to the West Indian Ocean, we observe a clear curvature bending towards the coastal western Sumatra, where the OLZ is evident at 2.2ºN (200 m depth) and 6.3ºS (700 m depth). The feature that causes a relatively higher DO concentration along the coastal western Sumatra may be driven by the SJUC.

4 Discussion

4.1 Sources of oxygen-depleted waters in the Sumatra-Java coasts

Our analyses of WOA and cruise-based data show seasonal variations in the imprints of oxygen-depleted northern Indian Ocean waters that are advected to the Sumatra-Java coasts by the regional ocean currents. To illustrate the mechanisms of the intrusion of the northern Indian Ocean waters, particularly from the saline Arabian Sea to the coasts of Sumatra and Java, Figure 5 shows salinity superimposed on currents at 100 to 1,000 m depths during both seasons. The oxygen-depleted Arabian Sea and the BoB waters are distinct in their salinities with high saline Arabian Sea and low saline BoB waters.

At the 100 m depth, the eastward propagating Equatorial Counter Current (ECC) is stronger during the boreal summer, thus delivering high saline low deoxygenated waters to the western Sumatra coast, which diminishes in the lower depths (Fig. 5-Right). The counter current reaches the eastern Indian Ocean and forms by the Somali Current from the north and the East African Coast Current from the south, thus feeding into the eastward equatorial currents (Sanchez-Franks et al., 2019; Schott and McCreary, 2001). A second of high saline waters is also observed as a result of an extended tongue of the Arabian Sea saline water via the Southwest Monsoon Current (SMC). The SMC, which flows from the Arabian Sea to the BoB through the south of Sri Lanka, is a surface-intensified current with a northward flow that reaches a depth of 300 m (Vinayachandran et al., 2018). Some currents continuously flow northward and bifurcate to the south reaching the coast of Sumatra.

https://doi.org/10.5194/egusphere-2024-451
Preprint. Discussion started: 28 February 2024

During the boreal winter, the South Equatorial Counter Current (SECC) at around 5ºS was essential for transferring highly saline water to the eastern Indian Ocean and subsequently into the southern coast of Java and Nusa Tenggara, where it mets the outflow of the ITF (Fig. 5-Left). At the eastern end of SECC, the SJC that flows southeastward along the coast of Sumatra and Java (Quadfasel and Cresswell, 1992; Iskandar et al., 2006), may play an important role in delivering SECC waters in the SETIO. The SJC is located in the upper 100 m, underneath the 200-1,000 m deep SJUC that carries a core of high saline and low oxygen North Indian Intermediate Water (Wijffels et al., 2002; Fieux et al., 2005). The SJC and SJUC signals flow eastward past the Savu Sea and reach the Ombai Strait as one of the major outflows of ITF (Sprintall et al., 2010). Salinity around the Sumatra-Java and Nusa Tenggara coasts varies, especially between 100 m and 200 m due to the dilution by ITF water. Additionally, the seawater freshening may have occurred westward at the Sunda Strait as a minor ITF outflow and subsequently expands due to wind stress and reversing currents in the Java-Sumatra coasts (Potemra et al., 2016; Susanto et al., 2016; Hamzah et al., 2020).

It is interesting to point out the role of the Wyrtki Jet along the equatorial Indian Ocean during the transition months in aiding the eastward transport of high salinity cores to the coasts of Sumatra and Java. The Wyrtki Jet, a strong eastward current along the equator caused by the presence of strong westerly winds, is prominent near the coasts of Sumatra and Java during the March-May and September-November months (Knaus and Taft, 1964; Wyrtki, 1973). As the western Indian Ocean thermocline lifted, the jet drives water masses with low oxygen and salinity maxima eastward while deepening in the west Sumatra mixed layer (see contour salinity of 35 PSS in the coastal region; Fig. 3). The jet changes direction below 120 m and is strongest between 60°E and 90°E at the surface. The EUC, which also flows eastward, is located beneath (Wyrtki, 1973). Furthermore, the SJC (200 m) and its deeper SJUC (200-1000 m), which has a reversal direction, redistribute these water masses throughout the Sumatra and Java coasts (Iskandar et al., 2006; Sprintall et al., 2010). These support the critical influence of the jet to distribute seawater masses in the region.

To further investigate the imprint of saline northern Indian Ocean and freshwater water masses in the SETIO, we assess the relationship between salinity and current zonal velocity in the equatorial (80.5°E, 3°N-3°S) and at the Sunda Strait outlet (107°E, 7.75-9.5°S) areas between 2000-2020 (Fig. 6). Salinity profiles corroborate that the western equatorial Indian Ocean is a major source of high (>35 PSS) saline waters, which are also consistent with those observed between 40-100°E along the equator. The eastward velocity centered at the subsurface at 100 m depth extends to 3°N and 3°S. In comparison, the observed high saline waters and eastward zonal velocity are constrained around the equator at the

https://doi.org/10.5194/egusphere-2024-451
Preprint. Discussion started: 28 February 2024

200 m depth. Our results agree with Argo float (ID #1901444) salinity data showing high saline waters in the upper 150 m of the eastern Indian Ocean. Salinity and zonal velocity experience drastic changes with the presence of saline water intrusion in certain years, i.e. 2007, 2015, and 2019. Of those events, the strongest one in 2019 is concurrent with the positive IOD event. Moreover, we observ a brief temporal lag between strong currents in the equatorial Indian Ocean and the emergence of high salinity waters in southern Java. Hence, we propose that the first baroclinic Kelvin waves are responsible for the observed zonal current changes off southern Java, consistent with previous works (Iskandar et al., 2006; Utari et al., 2019). By applying a lag correlation analysis, Utari et al. (2019) calculated an 18-day lag with an eastward propagating signal of a phase speed of around 2.37 m s^{-1}.

4.2 Shallow oxygen-depleted waters induced by upwelling

While lateral transports are essential in distributing low-deoxygenated water masses in the SETIO, the role of vertical advection such as upwelling events in the summer may be key in understanding deoxygenation via ocean dynamics and respiration of organic matters. Upwelling events could stimulate primary production increasing seawater oxygen contents and the subsequent export of organic materials that increases biological oxygen consumption (Pitcher et al., 2021). To elucidate the mechanisms by which upwelling may shape oxygen-depleted water in the upper ocean, we characterize subsurface waters upwelled into the surface using *in situ* data from the Argo floats, a RAMA buoy and cruise-based measurements (Fig. 7).

In situ temperature and salinity data provided by the Argo show clear seasonality and interannual variations. Saline (34.3 PSS) waters during the southeast summer monsoon accompanied by cool (27°C) temperatures, suggesting water originated from deeper depths (Figs. 7a and 7b). In addition to the significant impact of seasonality on changes in temperature and salinity, IOD events, most notably the 2019 positive IOD, caused a prolonged period of low seawater temperatures from the subsurface layers to the coasts of Sumatra and Java. The propagation of Kelvin waves from the equatorial Indian Ocean influences the extent and magnitude of upwelling in Java and Sumatra, while IOD and ENSO events both contribute to upwelling variations at the coast of Sumatra and Java (Vinayachandran et al., 2021). Further discussions on how interannual Indo-Pacific climate variations may shape oxygen concentrations at our study site are discussed in Section 4.3.

Two *in situ* oxygen measurements installed on a RAMA buoy at the surface (10 m) and subsurface (300 m) depths elucidate changes associated with the primary production and respiration of organic matters that modulate seawater DO (Fig. 7c). In the surface layer, oxygen levels are noticeably

https://doi.org/10.5194/egusphere-2024-451
Preprint. Discussion started: 28 February 2024

higher during the upwelling season that runs from June to October, due to biological production process involving phytoplankton photosynthesis. The temporal evolution of DO is consistent with changes in chlorophyll-a observed in the coasts of Sumatra and Java associated with upwelling (Susanto et al., 2006). Within the summer season, we observe short-term (~15-20 days) DO variations that the respiration of organic matter may drive. At 300 m depth, DO concentrations are consistently higher at the peak of the upwelling season (August-September), with another period of high DO values in the boreal winter. While the high DO content in the earlier may be driven by biological production, the high content during the latter may be associated with the ventilation from the ITF outflows. In some parts, DO at the 300 m depth reaches the OLZ level, indicating high oxygen consumption.

Observations from three stations located west to east in the south of Java during the July 2022 cruise indicate upwelling along the southern coast of Java that may be influenced by the ITF outflow. Coastal upwelling, indicated by relatively higher chlorophyll-a, is evident and more intense around St. 37 (Fig. 8a). This is further corroborated by lower temperatures and higher salinities in the surface depths at St.37, suggesting the presence of upward subsurface water into the surface (Fig. 8b). We also observe an interesting feature of curved high chlorophyll-a distribution that may indicate the role of the ITF outlet at the Lombok Strait, corroborated by the westward winds during the period. Earlier upwelling investigations have also shown the presence of upwelling that seems to be initiated at the southeastern tip of Java Island near St. 37 (Susanto et al., 2006; Iskandar et al., 2009; Mandal et al., 2022, Wirasatriya et al., 2020).

Comparative DO profiles from east to west, show higher DO content at the most eastward St. 37 while DO contents plummet to the 60 μmol kg^{-1} threshold at deeper depths towards the west, which lends support to the respiration of nutrient-rich surface waters driven by the easterly alongshore winds. The vertical DO profile does not detect any hypoxic area even at the subsurface depths despite upwelling occurring in the vicinity of St. 37 (Fig. 8c). The observation is consistent with the refilling by the ITF water from the outlet passage of Lombok Strait (Makarim et al., 2019). Towards the west, the hypoxic zone threshold (60 μmol kg^{-1}) is detected at shallower depths, which are ~400-700 m at St. 14 and ~180-800 m at the westernmost St. 04. The lowered DO content at St. 04 changed rapidly, suggesting strong remineralization of organic matters. More sinking organic matter from the Java Sea near St. 04 would promote low oxygen levels. Significantly low salinity water (33 PSS) at St. 04 supports the Java Sea water intrusion into the Indian Ocean through the Sunda Strait, therefore supplying significant levels of nutrients and carbon that are crucial for biological activity at the surface layer (Hamzah et al., 2020).

https://doi.org/10.5194/egusphere-2024-451
Preprint. Discussion started: 28 February 2024

4.3 Low and high-frequency changes in oxygen-depleted waters in the SETIO

The comparison between two observational stations located in western Sumatra (98ºE, 3ºS) and southern Java (107ºE, 7.75ºS) show consistent seasonal and interannual variations in both sites; however, with a clear secular trend towards deepened OLZ in western Sumatra (Figs. 9a and 9b). Along water depths of 120 to 200 m, prominent seasonal fluctuations in oxygen concentrations may be driven by the local monsoonal winds over the Indonesian maritime continent. During the early southeast monsoon in June, the alongshore wind grows more vigorous causing the thermocline to shoal. The pattern reaches its peak in July-August, consistent with cool sea surface temperature (SST) in the subsequent months. Simultaneously, low oxygen concentrations rise from the subsurface 200 m to the mixed layer during these summer months. In the deeper depths below 250 m, temporal changes in the OLZ show markedly different trends between the western Sumatra and southern Java areas. While the latter shows a slight trend toward deepened OLZ, the trend has been rather drastic since 2001. An OLZ of 60 mol kg^{-1} was found in 2001 at 600 m and remained marginally steady at 1000 m from 2012 to 2020. Our findings are comparable to previous studies that discovered a maximum salinity of 35.1 PSS and a minimum oxygen concentration of 53.6 mol kg^{-1} originating from the Arabian Sea and Red Sea Water along the Sumatra and Java coasts around 700-800 m (Coatanoan et al., 2010). Although our results show that oxygen concentrations of 60 µmol kg^{-1} persist at 800-900 m in southern Java, this low oxygen background indicates that the regulated factors and mechanisms in Java and Sumatra are slightly different.

DO concentrations in the thermocline depths of the SETIO are sensitive to the interannual positive ENSO variations with more constrained IOD impacts in the southern Java section (Figs. 9c and 9d). Unlike in the south of Java, DO variations in upper western Sumatra are less sensitive to interannual Indo-Pacific variations. Strong positive ENSO events (e.g., 2006, 2012, 2015, 2019) coincide with shoaled thermocline or lower oxygen levels in the southern Java section of the SETIO. Conversely, our data show that only the strong 2015 positive IOD event has a similar impact. In 2006, the positive IOD event in the Indian Ocean coincides with a positive ENSO event in the Pacific; thus, the observed lowered DO change in the SETIO may be more associated with ENSO as opposed to only IOD. Positive IOD is characterized by relatively higher sea surface height, causing lower SST and upwelled deoxygenated water to the surface. It is interesting to note that while previous works have shown strong IOD impacts on surface biogeochemistry, such as the distribution of the chlorophyll-a contents (e.g. Iskandar et al., 2009; Siswanto et al., 2020; Shi and Wang, 2021; Susanto et al., 2006),

https://doi.org/10.5194/egusphere-2024-451
Preprint. Discussion started: 28 February 2024

the imprint of positive IOD in the thermocline OLZ is much more muted as shown in our analyses. Indeed, chlorophyll has a distinct vertical distribution pattern, particularly in the oligotrophic ocean (Mignot et al., 2014; Barbieux et al., 2019; Xu et al., 2022), where the maximum concentration varies between 40-100 m in the global ocean (Yanusaka et al., 2022). During the negative IOD and ENSO events, for instance, in 2010, we observe that the OLZ threshold descends to a depth of ~180 m, which may be associated with downwelling off the coast of Java. Intense rainfall during the combined negative IOD and negative ENSO would increase organic matter from river discharges, thus further contributing to decreasing DO in the region. Taken together, we highlight the importance of chlorophyll-a and organic matter measurements not only in the surface ocean but also along the water column to comprehend the role of regional dynamics in ocean biogeochemistry.

5. Concluding remarks

Using available *in situ* and reanalysis data between 2010-2022, we detect the pervasiveness of oxygen-depleted northern Indian waters to the western Indonesian coasts in the SETIO, which our understanding of ocean deoxygenation is lacking. While the OLZ is present at various depths around the coasts of Sumatra and Java, the lower oxygen of ~40 μmol kg^{-1} is observed only in northwest Sumatra. Lateral currents in the equatorial Indian Ocean play a major role in delivering the oxygen-depleted high-salinity water masses with a prominent role of the eastward propagating Equatorial Counter Current during the boreal summer, the SECC in the winter and the Wyrtki Jet during the transition months. Our analyses corroborate that the first baroclinic Kelvin waves may play a role in the emergence of high-salinity waters in southern Java. While lateral transports are important in delivering the low-deoxygenated water masses to the SETIO, coastal upwelling events driven by easterly winds during the boreal summer stimulate the biological oxygen production and subsequently the respiration of organic matters at intermediate depths (200-1,000 m) as the water mass being advected westward from the southeastern coast of Java towards Sumatra. The outflow of fresh Indonesian Throughflow in the Indian Ocean via the Lombok and Sunda Straits further modifies the local distribution of low-deoxygenated water mass along the coast of Sumatra and Java, and lowers the oxygen level further due to the additional input of organic matter from the Indonesian maritime continent. High-resolution biogeochemical measurements are critical to understanding changes in the regional DO in different seasons.

In conclusion, the pervasiveness of low-deoxygenated northern Indian waters indicated by a clear secular trend towards deepened OLZ in western Sumatra highlights the importance of long

https://doi.org/10.5194/egusphere-2024-451
Preprint. Discussion started: 28 February 2024

observational data across depth profiles in the SETIO. Unlike in southern Java, DO variations in upper western Sumatra are less sensitive to interannual Indo-Pacific variation. The imprints of the Indo-Pacific climate variations to DO concentrations are evident in the thermocline depths of southern Java, intriguingly, with stronger positive ENSO imprints (e.g. 2006, 2012, 2015, 2019) compared to positive IOD events. Only the strong 2015 positive IOD event shows a clear impact on DO in the SETIO.

https://doi.org/10.5194/egusphere-2024-451
Preprint. Discussion started: 28 February 2024

Appendix

A. Cruise Description

Appendix Table A1. Brief on field campaigns in the southern coast of Java used in this study.

Cruise	Description
Java Upwelling Variation Observation (JUVO)	JUVO was a collaborative program between the Ministry of Marine Affairs and Fisheries and the First Institute of Oceanography (FIO) to understand Java upwelling variability. The program deployed a subsurface mooring system consisting of an ADCP and CTD sensors at various depths to obtain velocity, temperature, and salinity profiles.
Monsoon Onset Monitoring, Its Social and Ecosystem Impacts (MOMSEI)	MOMSEI was a regional program initiated by the Intergovernmental Ocean Commission Western Pacific Sub-Commission (IOC/WESTPAC) to understand the monsoonal upwelling and its climate and ecosystem impacts.
TRansport Indonesian seas, Upwelling and Mixing Physics (TRIUMPH)	TRIUMPH was an international collaboration between the Indonesian Institute of Sciences (LIPI) now the National Research and Innovation Agency (BRIN), FIO and the University of Maryland, to understand IOD variability in the eastern Indian Ocean and upwelling.
Expedition of Widya Nusantara (EWIN)	BRIN's EWIN cruise conducted in the Indian Ocean made oceanographic observations to understand the impact on marine productivity and biogeochemistry.

https://doi.org/10.5194/egusphere-2024-451
Preprint. Discussion started: 28 February 2024

466 **B. Model Validation**

467 **Appendix Table A2.** RRMSE and MAPE values at measurement stations in southern Java.

Station ID	RRMSE (%)	MAPE (%)
St. 04	17.23	15.25
St. 13	7.93	7.22
St. 14	8.70	8.34

468

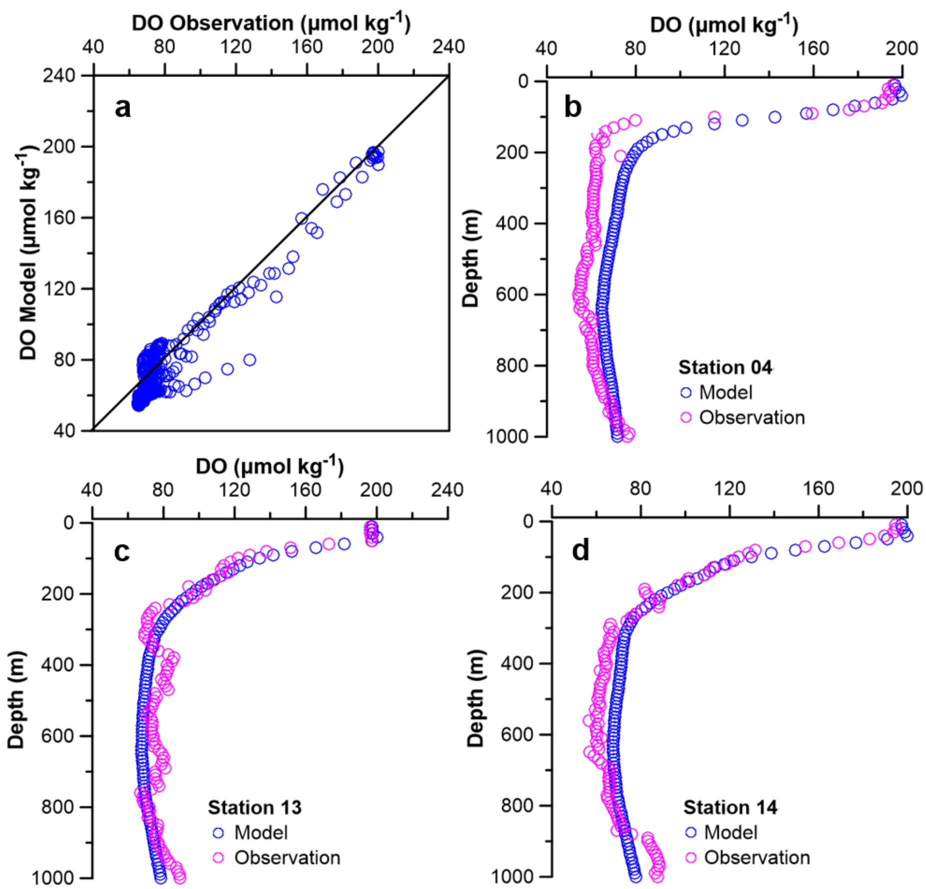

469

470 **Appendix Figure A1**. (a) The comparison between DO concentration from observation and model
471 (μmol kg^{-1}) in southern Java. (b) Vertical profiles of DO concentration (model and observation) during
472 the 2022 cruise at St. 04, (c) St. 13, and (d) St. 14.

https://doi.org/10.5194/egusphere-2024-451
Preprint. Discussion started: 28 February 2024

Data Availability

- Cruise-based CTD and DO data presented herein are deposited at the Repositori Ilmiah Nasional (RIN): https://data.brin.go.id/dataset.xhtml?persistentId=hdl:20.500.12690/RIN/KWW79C.
- Argo temperature and salinity data (ID #1901444 and #5905017): http://www.argodatamgt.org/Access-to-data/Argo-data-selection.
- RAMA buoy CTD and DO data: https://www.pmel.noaa.gov/tao/drupal/rama-display.
- WOA18 DO and salinity data: https://www.ncei.noaa.gov/access/world-ocean-atlas-2018.
- Copernicus Marine Environment Monitoring Service (CMEMS) salinity, ocean current and DO data: https://data.marine.copernicus.eu/products.
- NOAA chlorophyll-a and wind stress data: https://coastwatch.pfeg.noaa.gov/erddap/index.html.
- NOAA Ocean Observations Panel for Climate's IOD and Niño 3.4 indices: https://gcos.wmo.int/en/home.

Author Contributions

FH, IT, AS, and ISN conceptualized the paper, and developed the framework and key messages. FH, AS, BP, DB, MF, RDAO, TA, MJR and PDS conducted data compilation and analyses. FH, IT, AS, ISN, MF, RDAO, DB, WY, ZW, HW, RDS and PDS wrote manuscript, reviewed and edited the manuscript. All authors have discussed and reviewed the manuscript, conducted manuscript proofreading, and approved the final version of the manuscript.

Competing Interests

The contact author has declared that none of the authors has any competing interests.

Acknowledgements

We thank the crews of the RV Baruna Jaya I, RV Baruna Jaya III, RV Baruna Jaya VIII, and RV Madidihang 03 for their instrumental assistance to the research cruises conducted between 2011-2022.

Financial Support

This work was funded by the Indonesian Ministry of Marine Affairs and Fisheries (KKP) and the First Institute of Oceanography (FIO) through the JUVO Project (2011-2016) and the MOMSEI Project (2013); the Indonesian Institute of Sciences now the National Research and Innovation Agency Indonesia (BRIN), FIO, and University of Maryland (UMD) through the TRIUMPH Project (2018-

2022), BRIN Sailing Day (#2307/II.7/HK.01.00/6/2022) (2022); RDS was supported by the National Aeronautics and Space Administration (NASA) through the UMD Grant #80NSSC18K0777. ZW was jointly funded by the Laoshan Laboratory (contract #LSKJ202202700), the National Natural Science Foundation of China (grant #42076024) and the China-ASEAN Blue Partnership Construction Program.

References

Al Azhar, M., Lachkar, Z., Lévy, M., and Smith, S.: Oxygen minimum zone contrasts between the Arabian Sea and the Bay of Bengal implied by differences in remineralization depth, Geophys. Res. Lett., 44:11, 106–114, https://10.1002/2017GL075157, 2017.

Aumont, O., Éthé, C., Tagliabue, A., Bopp, L., and Gehlen, M.: PISCES-v2 an ocean biogeochemical model for carbon and ecosystem studies, Geoscientific Mod. Dev. Dis., 8:2, 2465–2513. https://doi.org/10.5194/gmd-8-2465-2015, 2015.

Ayers, J. M., Strutton, P. G., Coles, V. J., Hood, R. R., and Matear, R. J.: Indonesian throughflow nutrient fluxes and their potential impact on Indian Ocean productivity, Geophys. Res. Lett., 41, 5060–5067, https://doi.org/10.1002/2014GL060593, 2014.

Barbieux, M., Uitz, J., Gentili, B., Pasqueron de Fommervault, O., Mignot, A., Poteau, A., Schmechtig, C., Taillandier, V., Leymarie, E., Penkerc'h, C., d'Ortenzio, F., Claustre, H., and Bricaud, A.: Bio-optical characterization of subsurface chlorophyll maxima in the Mediterranean Sea from a Biogeochemical-Argo float database. Biogeosciences, 16, 1321–1342, https://doi.org/10.5194/bg-16-1321-2019, 2019.

Breitburg, D., Levin, L. A., Oschlies, A., Grégoire, M., Chavez, F. P., Conley, D. J., Garçon, V., Gilbert, D., Gutiérrez, D., Isensee, K., Jacinto, G.S., Limburg, K. E., Montes, I., Naqvi, S.W. A., Pitcher, G. C., Rabalais, N. N., Roman, M. R., Rose, K. A., Seibel, B. A., Telszewski, M., Yasuhara, M., and Zhang, J.: Declining oxygen in the global ocean and coastal waters, Science, 359:6371, 1-11, https://doi.org/10.1126/science.aam7240, 2018.

Bindoff, N. L., Cheung, W. W. L., Kairo, J. G., Arístegui, J., Guinder, V. A., Hallberg, R., Hilmi, N., Jiao, N., Karim, M. S., Levin, L., O'Donoghue, S., Purca Cuicapusa, S. R., Rinkevich, B., Suga, T., Tagliabue, A., and Williamson, P.: Changing ocean, marine ecosystems, and dependent communities, In: Special report on ocean and cryosphere in a changing climate, Intergovernmental Panel on Climate Change, Geneva. IPCC report 2019, edited by: Pörtner H. -O., Roberts, D, C.,

https://doi.org/10.5194/egusphere-2024-451
Preprint. Discussion started: 28 February 2024

Masson-Delmotte, V., Zhai, P., Tignor, M., Poloczanska, E., Mintenbeck, A., Alegria, A., Nicolai, M., Okem, A., Petzold, J., Rama, B., and Weyer, N. M, IPCC Report, 2019.

Canadell, J. G., Monteiro, P. M. S., Costa, M. H., Cotrim da Cunha, L., Cox, P. M., Eliseev, A. V., Henson, S., Ishii, M., Jaccard, S., Koven, C., Lohila, A., Patra, P. K., Piao, S., Rogelj, J., Syampungani, S., Zaehle, S., and Zickfeld, K.: Global Carbon and other Biogeochemical Cycles and Feedbacks, In: Climate Change 2021: The Physical Science Basis, edited by: Masson-Delmotte, V., Zhai, P., Pirani, A., Connors, S. L., Péan, C., Berger, S., Caud, N., Chen, Y., Goldfarb, L., Gomis, M.I., Huang, M., Leitzell, K., Lonnoy, E., Matthews, J. B. R., Maycock, T. K., Waterfield, T., Yelekçi, O., Yu, R., and Zhou, B., Cambridge University Press, Cambridge, United Kingdom and New York, 673–816, https://doi.org/10.1017/9781009157896.007, 2021.

Coatanoan, C., Metzl, N., Fieux, M., and Coste, B.: Seasonal water mass distribution in the Indonesian Throughflow entering the Indian Ocean, J. Geophys. Res., 104:C9, 20801-20826, https://doi.org/10.1029/1999JC900129, 1999.

Diaz, R. J., and Rosenberg, R.: Spreading dead zones and consequences for marine ecosystems, Science, 321:5891, 926-929, https://doi.org/10.1126/science.1156401, 2008.

Espinosa-Díaz, L. F., Zapata-Rey, Y. T., Ibarra-Gutierrez, K., Bernal, C. A.: Spatial and temporal changes of dissolved oxygen in waters of the Pajarales complex, Ciénaga Grande de Santa Marta: Two decades of monitoring, Sci. of The Total Enviro., 785:147203, https://doi.org/10.1016/j.scitotenv.2021.147203, 2021.

Fieux, M., Molcard, R., Morrow, R.: Water properties and transport of the Leeuwin Current and Eddies off Western Australia, Deep Sea Part I: Oceanographic Research Papers, 52:9, 1617-1635, https://doi.org/10.1016/j.dsr.2005.03.013, 2005.

Garcia, H. E., Weathers, K. W., Paver, C. R., Smolyar, I., Boyer, T. P., Locarnini, R. A., Zweng, M. M., Mishonov, A.V., Baranova, O. K., Seidov, D., and Reagen, J. R.: World Ocean Atlas 2018 Vol 4: Dissolved Inorganic Nutrients (phosphate, nitrate and nitrate+nitrite, silicate), A. Mishonov Technical Editor, NOAA Atlas NESDIS 84, 35pp, 2019.

Gilbert, D., Rabalais, N. N., Dıaz, R. J., and Zhang, J.: Evidence for greater oxygen decline rates in the coastal ocean than in the open ocean, Biogeosciences, 7, 2283–2296, https://doi.org/10.5194/bg-7-2283-2010, 2010.

Gordon, A. L., Ma, S., Olson, D. B., Hacker, P., Ffield, A., Talley, L. D., Wilson, D., and Baringer, M.: Advection and diffusion of Indonesian throughflow water within the Indian Ocean South

https://doi.org/10.5194/egusphere-2024-451
Preprint. Discussion started: 28 February 2024

Equatorial Current. Geophys. Res. Lett., 24:21, 2573–2576, https://doi.org/10.1029/ 97GL01061, 1997.

Hamzah, F., Agustiadi, T., Susanto, R. D., Wei, Z., Guo, L., Cao, Z., and Dai, M.: Dynamics of the carbonate system in the Western Indonesian Seas during the southeast monsoon, J. of Geophys. Res.: Oce., 125:1, https://doi.org/10.1029/2018JC014912, 2020.

Hamme, R. C., and Keeling, R. F.: Ocean ventilation as a driver of interannual variability in atmospheric potential oxygen, Tellus B: Chem. and Phys. Meteorology, 60:5, 706-717, https://doi.org/10.1111/j.1600-0889.2008.00376.x, 2008.

Helm, K. P., Bindoff, N. L., and Church, J. A.: Observed decreases in oxygen content of the global ocean, Geophys. Res. Lett., 38:23, 1-6, https://doi.org/10.1029/2011GL049513, 2011.

Helly, J. J., and Levin, L. A.: Global distribution of naturally occurring marine hypoxia on continental margins, Deep-Sea Research I: Ocean. Res. Papers, 51:9, 1159–1168, 2004.

Iskandar, I., Tozuka, T., Sasaki, H., Masumoto, Y., and Yamagata, T.: Intraseasonal variations of surface and subsurface currents off Java as simulated in a high resolution ocean general circulation model, J. Geophys. Res., 111:C12, 1-15, https://doi.org/10.1029/2006JC003486, 2006.

Iskandar, I., Rao, S. A., and Tozuka, T.: Chlorophyll-a bloom along the southern coasts of Java and Sumatra during 2006, Inter. J. of Rem. Sens., 30:3, 663-671, https://doi.org/10.1080/01431160802372309, 2009.

Ito, T., Minobe, S., Long, M. C., and Deutsch, C.: Upper ocean O_2 trends: 1958–2015, Geophys. Res. Lett., 44:9, 4214– 4223, https://doi.org/10.1002/2017GL073613, 2017.

Karstensen, J., Stramma, L., and Visbeck, M.: Oxygen minimum zone in the Eastern Tropical Atlantic and Pacific Oceans, Prog. in Oceano., 77:4, 331-350, https://doi.org/10.1016/j.pocean.2007.05.009, 2008.

Keeling, R. F., Körtzinger, A., Gruber, N.: Ocean deoxygenation in a warming world, Annu. Rev. Mar. Sci., 2, 199-229, https://doi.org/10.1146/annurev.marine.010908.163855, 2010.

Mignot, A., Claustre, H., Uitz, J., Poteau, A., D'Ortenzio, F., Xing, X.: Understanding the seasonal dynamics of phytoplankton biomass and the deep chlorophyll maximum in oligotrophic environments: a bio-argo float investigation, Glo. Biogeochem. Cycl., 28:8, 856–876, https://doi.org/10.1002/2013GB004781, 2014.

Mandal, S., Susanto, R. D., and Balaji, R.: Dynamical factors modulating surface chlorophyll-a variability along South Java Coast, Remote Sens., 14:7, 1745. https://doi.org/10.3390/rs14071745, 2022.

https://doi.org/10.5194/egusphere-2024-451
Preprint. Discussion started: 28 February 2024

Makarim, S., Sprintall, J., Liu, Z., Yu, W., Santoso, A., Yan, X. H., and Susanto, R. D.: Previously unidentified Indonesian Throughflow pathways and freshening in the Indian Ocean during recent decades, Sci. Rep., 9:7364, https://doi.org/10.1038/s41598-019-43841-z, 2019.

McCreary Jr, J. P., Yu, Z., Hood, R. R., Vinaychandran, P. N., Future, R., Ishida, A., and Richards, K. J.: Dynamics of the Indian-Ocean oxygen minimum zones, Prog. Oceanogr., 112, 15–37, https://doi.org/10.1016/j.pocean.2013.03.002, 2013.

McPhaden, M. J., Wang, Y., and Ravichandran, M.: Volume transports of the Wyrtki jets and their relationship to the Indian Ocean Dipole, J. Geophys. Res. Oceans, 120:8, 5302–5317, https://doi.org/10.1002/2015JC010901, 2015.

Moreno, J. J. M., Pol, A. P., Abad, A. S., and Blasco, B. C.: Using the R-MAPE index as a resistant measure of forecast accuracy, Psicothema, 25:4, 500-506. https://doi.org/10.7334/psicothema2013.23, 2013.

Naqvi, S. W. A., Naik, H., Jayakumar, D. A., Shailaja, M. S., and Narvekar, P. V.: Seasonal oxygen deficiency over the western continental shelf of India, Past and Present Water Column Anoxia, in Neretin, L. N., NATO Science Series IV Earth and Environmental Sciences, Springer, 64, 195–224. https://doi.org/10.1007/1-4020-4297-3_08, 2006.

Naqvi, S. W. A., Moffett, J. W., Gauns, M. U., Narvekar, P. V., Pratihary, A. K., Naik, H., Shenoy, D. M., Jayakumar, D. A., Goepfert, T. J., Patra, P. K., Al-Azri, A., and Ahmed, S. I.: The Arabian Sea as a high-nutrient, low-chlorophyll region dur- ing the late Southwest Monsoon, Biogeosciences, 7, 2091–2100. https://doi.org/10.5194/bg-7-2091-2010, 2010.

Oschlies, A., Schulz, K. G., Riebesell, U., and Schmittner, A.: Simulated 21st century's increase in oceanic suboxia by CO2-enhanced biotic carbon export, Glo. Biogeochem. Cyc., 22:4, GB4008, https://doi.org/10.1029/2007GB003147, 2008.

Paulmier, A., and Ruiz-Pino, D.: Oxygen minimum zones (OMZs) in the modern ocean, Prog. Oceanogr., 80:3-4, 113–128, https://doi.org/10.1016/j.pocean.2008.08.001, 2009.

Phillips, H. E., Tandon, A., Furue, R., Hood, R., Ummenhofer, C. C., Benthuysen, J. A., Menezes, V., Hu, S., Webber, B., Sanchez-Franks, A., Cherian, D., Shroyer, E., Feng, M., Wijesekera, H., Chatterjee, A., Yu, L., Hermes, J., Murtugudde, R., Tozuka, T., Su, D., Singh, A., Centurioni L,, Prakash, S., and Wiggert, J.: Progress in understanding of Indian Ocean circulation, variability, air-sea exchange and impacts on biogeochemistry, Ocean Sci., 17:6, 1677–1751, https://doi.org/10.5194/os-2021-1, 2021.

https://doi.org/10.5194/egusphere-2024-451
Preprint. Discussion started: 28 February 2024

Potemra, J. T., Hacker, P. W., Melnichenko, O., and Maximenko, N.: Satellite estimate of freshwater exchange between the Indonesian Seas and the Indian Ocean via the Sunda Strait, J. Geophys. Res. Oceans, 121:7, 5098– 5111, https://doi.org/10.1002/2015JC011618, 2016.

Poupon, M. A., Resplandy, L., Lévy, M., Bopp, L.: Pacific decadal oscillation influences tropical oxygen minimum zone extent and obscures anthropogenic changes, Geoph. Res. Lett., 50:7, https://doi.org/10.1029/2022GL102123, 2023.

Pitcher, G. C., Aguirre-Velarde, A., Breitburg, D., Cardich, J., Carstensen, J., Conley, D. J., Dewitte, B., Engel, A., Espinoza-Morriberón, D., Flores, G., Garçon, V., Graco, M., Grégoire, M., Gutiérrez, D., Hernandez-Ayon, J. M., Huang, H. H. M., Isensee, K., Jacinto, M. E., Levin, L., Lorenzo, A., Machu, E., Merma, L., Montes, I., SWA, N., Paulmier, A., Roman, M., Rose, K., Hood, R., Rabalais, N. N., Salvanes, A. G. V., Salvatteci, R., Sánchez, S., Sifeddine, A., Tall, A. W., Van der Plas, A. K., Yasuhara, M., Zhang, J., and Zhu, Z. Y.: System controls of coastal and open ocean oxygen depletion, Prog. in Ocean., 197, https://doi.org/10.1016/j.pocean.2021.102613, 2021.

Quadfasel, D., and Cresswell, G. R.: A note on the seasonal variability of the South Java Current, J. Geophys. Res. Oceans, 97:C3, 3685–3688, https://doi.org/10.1029/91JC03056, 1992.

Rahaman, A., Srinivasu, U., Panickal, S., Durgadoo, J. V., Griffies, S. M., Ravichandran, M., Bozec, A., Cherchi, A., Voldoire, A., Sidorenko, D., Chassignet, E. P., Danabasoglu, G., Tsujino, H., Getzlaff, K., Ilicak, M., Bentsen, M., Long, M. C., Fogli, P. G., Farneti, R., Danilov, S., Marsland, S. J., Valcke, S., Yeager, S. G., and Wang, Q.: An assessment of the Indian Ocean mean state and seasonal cycle in a suite of interannual CORE-II simulations, Oce. Model., 145, https://doi.org/10.1016/j.ocemod.2019.101503, 2020.

Rao, C. K., Naqvi, S.W.A., Kumar, M. D., Varaprasad, S. J. D., Jayakumar, D. A., George, M. D., and Singbal, S. Y. S.: Hydrochemistry of the Bay of Bengal Possible reasons for a different water-column cycling of carbon and nitrogen from the Arabian Sea, Mar. Chem., 47:3-4, 279–290, http://doi.org/10.1016/0304-4203(94)90026-4, 1994.

Reppin, J., Schott, F. A., Fischer, J., and Quadfasel, D.: Equatorial currents and transports in the upper central Indian Ocean Annual cycle and interannual variability, J. of Geophy. Res., 104:C7, 15495-15514, 1999.

Rixen, T., Cowie, G., Gaye, B., Goes, J., do Rosário Gomes, H., Hood, R. R., Lachkar, Z., Schmidt, H., Segschneider, J., and Singh, A.: Reviews and syntheses: Present, past, and future of the oxygen minimum zone in the northern Indian Ocean, Biogeosciences, 17, 6051–6080, https://doi.org/10.5194/bg-17-6051-2020, 2020.

Sanchez-Franks, A., Webber, B. G. M., King, B. A., Vinayachandran, P. N., Matthews, A. J., Sheehan, P. M. F., Behara, A., and Neema, C. P.: The railroad switch effect of seasonally reversing currents on the Bay of Bengal high-salinity core, Geophys. Res. Lett., 46:11, 6005– 6014, https://doi.org/10.1029/2019GL082208, 2019.

Sarma, V. V. S. S., Bhaskar, T. V. S. U., Kumar, J. P., and Chakraborty, K.: Potential mechanisms responsible for occurrence of core oxygen minimum zone in the north-eastern Arabian Sea, Deep Sea Research Part I: Oceanographic Research Papers, 16, https://doi.org/10.1016/j.dsr.2020.103393, 2020.

Schott, F. A., and McCreary Jr. J. P.: The Monsoon circulation of the Indian Ocean, Prog. in Ocean., 51:1, 1-123, https://doi.org/10.1016/S0079-6611(01)00083-0, 2001.

Schmidtko, S., Stramma, L., and Visbeck, M.: Decline in global oceanic oxygen content during the past five decades, Nature, 542, 335–339, https://doi.org/10.1038/nature21399, 2017.

Shenoy, D. M., Suresh, I., Uskaikar H., Kurian, S., Vidya, P. J., Shirodkar, G., Gauns, M. U., and Naqvi, S. W. A.: Variability of dissolved oxygen in the Arabian Sea Oxygen Minimum Zone and its driving mechanisms, J. Marine Syst., 204, https://doi.org/10.1016/j.jmarsys.2020.103310, 2020.

Shi, W., and Wang, M.: A biological Indian Ocean Dipole event in 2019, Sci. Rep., 11:2452, https://doi.org/10.1038/s41598-021-81410-5, 2021.

Siswanto, E., Horii, T., Iskandar, I., Gaol, J. L., Setiawan, R. Y., and Susanto, R. D.: Impacts of climate changes on the phytoplankton biomass of the Indonesian Maritime Continent, J. Mar. Sys., 212, https://doi.org/10.1016/j.jmarsys.2020.103451, 2020.

Susanto, R. D., Moore II, T. S., and Marra, J.: Ocean color variability in the Indonesian Seas during the SeaWiFS Era, Geochemistry Geophysics Geosystems, 7:5, https://doi.org/10.1029/2005GC001009, 2006.

Susanto, R. D., Wei, Z., Adi, T. R., Zheng, Q., Fang, G., Fan, B., Supangat, A., Agustiadi, T., Li, S., Trenggono, M., and Setiawan, A.: Oceanography Surrounding Krakatau Volcano in the Sunda Strait, Indonesia, Oceanography, 29:2, 264–272, http://www.jstor.org/stable/24862689, 2016.

Sprintall, J., Chong, J., Syamsudin, F., Morawitz, W., Hautala, S., Bray, N., and Wijffels, S.: Dynamics of the South Java Current in The Indo-Australian Basin, Geophys. Res. Lett., 26:16, 2493-2496, https://doi.org/10.1029/1999GL002320, 1999.

https://doi.org/10.5194/egusphere-2024-451
Preprint. Discussion started: 28 February 2024

Sprintall, J., Wijffels, S., Molcard, R., and Jaya, I.: Direct evidence of the South Java Current system in Ombai Strait. Dyn. Atmos. and Oce., 50:2, 140-156, https://doi.org/10.1016/j.dynatmoce.2010.02.006, 2010.

Swallow, J. C.: Some Aspects of the Physical Oceanography of the Indian Ocean, Deep Sea Research Part A: Ocean. Res. Papers, 31:6-8, 639-650, https://doi.org/10.1016/0198-0149(84)90032-3, 1984.

Talley, L. D., and Sprintall, J.: Deep expression of the Indonesian Throughflow: Indonesian Intermediate Water in the South Equatorial Current, J. Geophy. Res., 110:C10, https://doi.org/10.1029/2004JC002826, 2005.

Utari, P. A., Setiabudidaya, D., Khakim, M. Y. N., and Iskandar, I.: Dynamics of the South Java Coastal Current revealed by RAMA observing network, Terr. Atmos. Ocean. Sci., 30, 235-245, https://doi.org/10.3319/TAO.2018.12.14.01, 2019.

Vaquer-Sunyer, R., and Duarte, C. M.: Threshold of Hypoxia for Marine Biodiversity, PNAS, 105:40, 15452-15457, https://doi.org/10.1073/pnas.0803833105, 2008.

Valcheva N., and Palazov A.: Quality control of CTD observations as a basis for estimation of thermohaline climate of the western black sea, J. Env. Prot. and Eco., 11:4, 1504–1515, 2010.

Vinayachandran, P. N., Matthews, A. J., Kumar, K. V., Sanchez-Franks, A., Thushara, V., George, J., Vijith, V., Webber, B. G. M., Queste, B. Y., Roy, R., Sarkar, A., Baranowski, D. B., Bhat, G. S., Klingaman, N. P., Peatman, S. C., Parida, C., Heywood, K. J., Hall, R., King, B., Kent, E. C., Nayak, A. A., Neema, C. P., Amol, P., Lotliker, A., Kankonkar, A., Gracias, D. G., Vernekar, S., D'Souza, A. C., Valluvan, G., Pargaonkar, S. M., Dinesh, K., Giddings, J., and Joshi, M.: BoBBLE: Ocean–Atmosphere Interaction and Its Impact on the South Asian Monsoon, Bulletin of the American Met. Soc., 9:8, 1569-1587, https://doi.org/10.1175/BAMS-D-16-0230.1, 2018.

Wirasatriya, A., Setiawan, J. D., Sugianto, D. N., Rosyadi, I. A., Haryadi, H., Winarso, G., Setiawan, R. Y., and Susanto, R. D.: Ekman dynamics variability along the southern coast of Java revealed by satellite data, Inter. J. Rem. Sens., 41:21, 8475-8496, https://doi.org/10.1080/01431161.2020.1797215, 2020.

Wijffels, S., Sprintall, J., Fieux, M., and Bray, N.: The JADE and WOCE I10/IR6 Throughflow sections in the southeast Indian Ocean. Part 1: water mass distribution and variability, Deep Sea Res. Part II: Tropical Studies in Ocean., 49:7-8, 1341–1362. https://doi.org/10.1016/S0967-0645(01)00155-2, 2002.

https://doi.org/10.5194/egusphere-2024-451
Preprint. Discussion started: 28 February 2024

Wyrtki, K.: The Oxygen Minima in Relation to Ocean Circulation, Deep Sea Res. and Ocean. Abstr., 9:1-2, 11-23, https://doi.org/10.1016/0011-7471(62)90243-7, 1962.

Wyrtki, K.: An Equatorial Jet in the Indian Ocean, Science, 181:4096, 262-264. https://doi.org/10.1126/science.181.4096.262, 1973.

Xu, W., Wang, G., Cheng, X., Jiang, L., Zhou, W., and Cao, W.: Characteristics of subsurface chlorophyll maxima during the boreal summer in the South China Sea with respect to environmental properties, Sci. Total Environ., 820,https://doi.org/10.1016/j.scitotenv.2022.153243, 2022.

Yang, G., Zhao, X., Li, Y., Liu, L., Wang, F., and Yu, W.: Chlorophyll variability induced by mesoscale eddies in the southeastern tropical Indian Ocean. J. Mar. Sys., 199, https://doi.org/10.1016/j.jmarsys.2019.103209, 2019.

You, Y., and Tomczak, M.: Thermocline circulation and ventilation in the Indian Ocean derived from water mass analysis, Deep Sea Research Part 1: Ocean. Res. Papers, 40:1, 13-56, https://doi.org/10.1016/0967-0637(93)90052-5, 1993.

Yasunaka, S., Ono, T., Sasaoka, K., and Sato, K.: Global distribution and variability of subsurface chlorophyll a concentration, Ocean Sci., 18:1, 255–268, https://doi.org/10.5194/os-18-255-2022, 2022.

https://doi.org/10.5194/egusphere-2024-451
Preprint. Discussion started: 28 February 2024

Figures

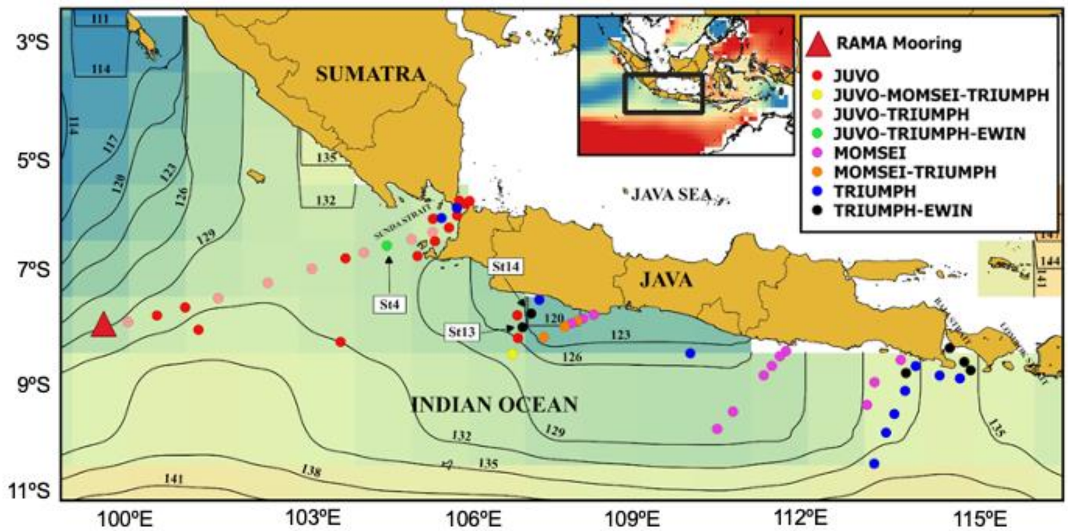

Figure 1. Study area showing sampling stations during international cruise campaigns between 2010-2022 (color dots) and a RAMA buoy (red triangle). DO data from St. 04, St. 13 and St. 14 in the 2022 cruise are used for the model validation. The contours mark DO concentration (µmol kg^{-1}) at a 100 m depth.

https://doi.org/10.5194/egusphere-2024-451
Preprint. Discussion started: 28 February 2024

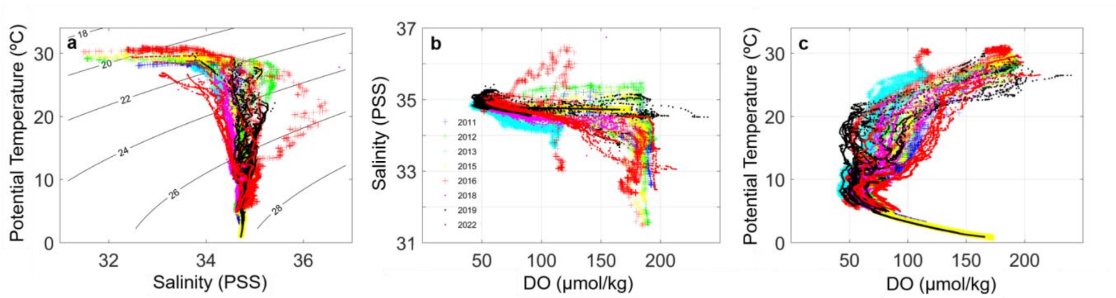

Figure 2. Relationships between potential temperature, salinity and DO at compiled stations of the 2010-2022 cruises.

https://doi.org/10.5194/egusphere-2024-451
Preprint. Discussion started: 28 February 2024

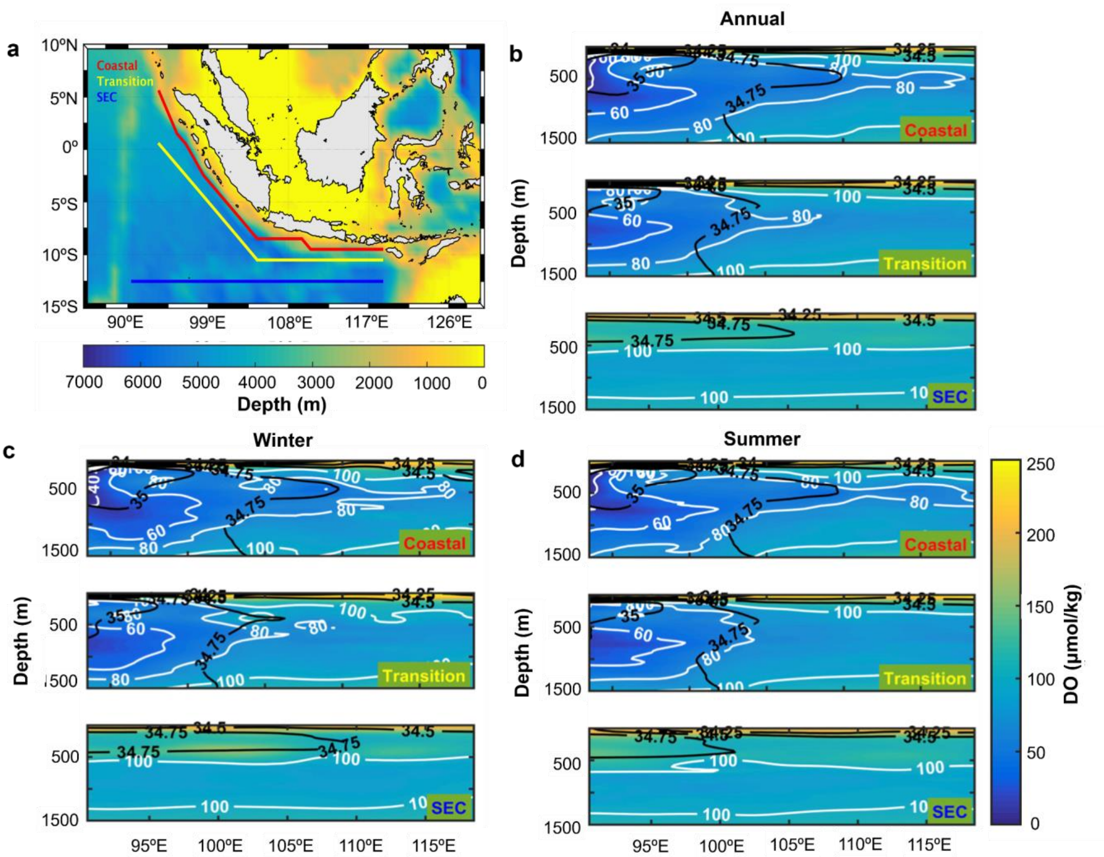

Figure 3. (a) DO concentrations along the coastal (red), transition (yellow), and SEC (blue) cross-sections. **(b)** Annual climatology DO. **(c)** Boreal winter (Jan-Mar) climatology DO. **(d)** Boreal summer (July-Sept) climatology DO. The white and black contours mark DO and 34-35.5 PSS isohalines, respectively. DO and salinity data of WOA18.

https://doi.org/10.5194/egusphere-2024-451
Preprint. Discussion started: 28 February 2024

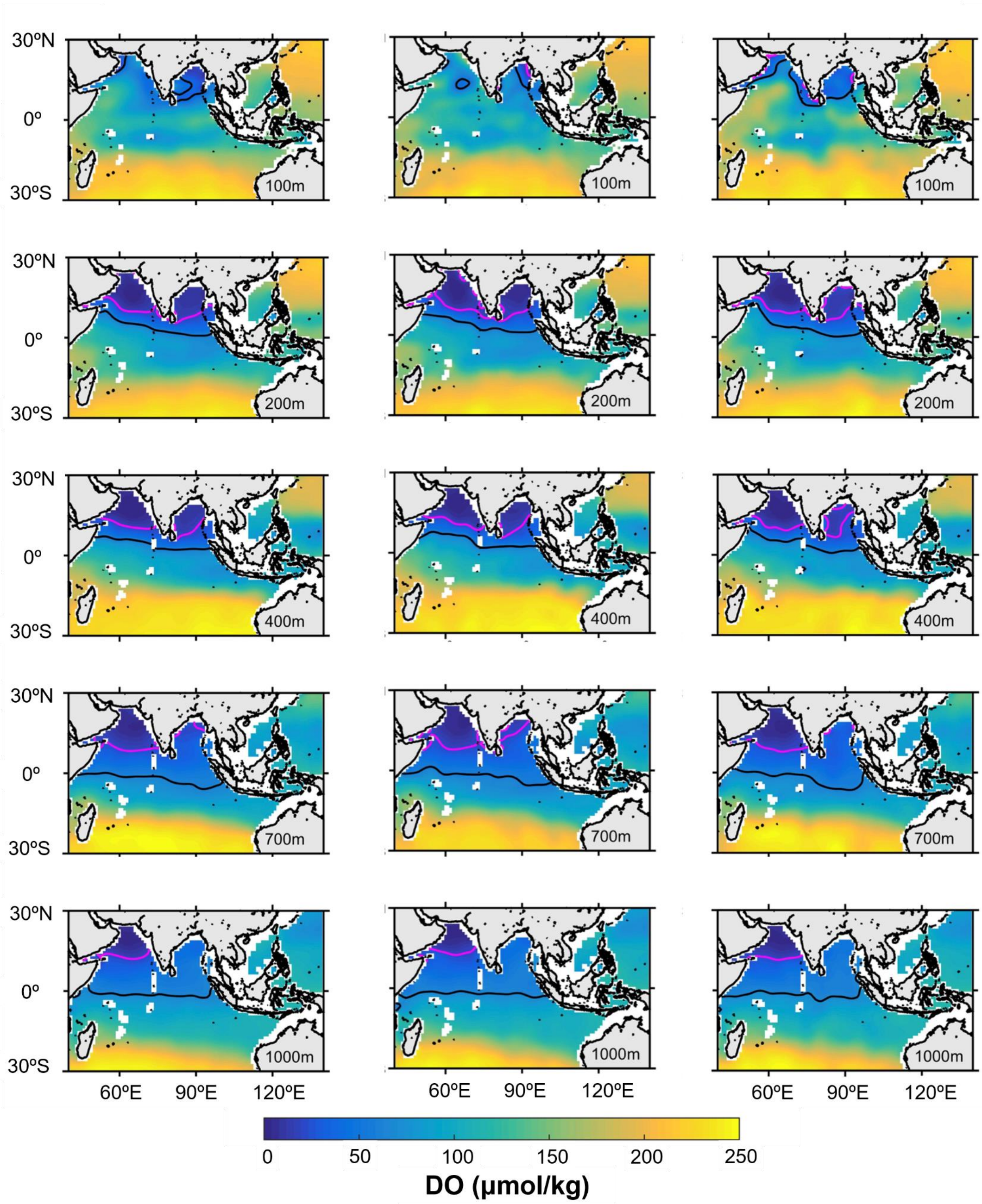

Figure 4. (Left) Annual climatology DO concentrations across depths at 100, 200, 400, 700 and 1,000 m. **(Center)** Boreal winter (Jan-Mar) climatology DO. **(Right)** Boreal summer (July-Sept) climatology DO. The black and purple lines denote the OLZ (DO=60 μmol kg^{-1}) and the OMZ (DO=22 μmol kg^{-1}), respectively. DO data of WOA18.

https://doi.org/10.5194/egusphere-2024-451
Preprint. Discussion started: 28 February 2024

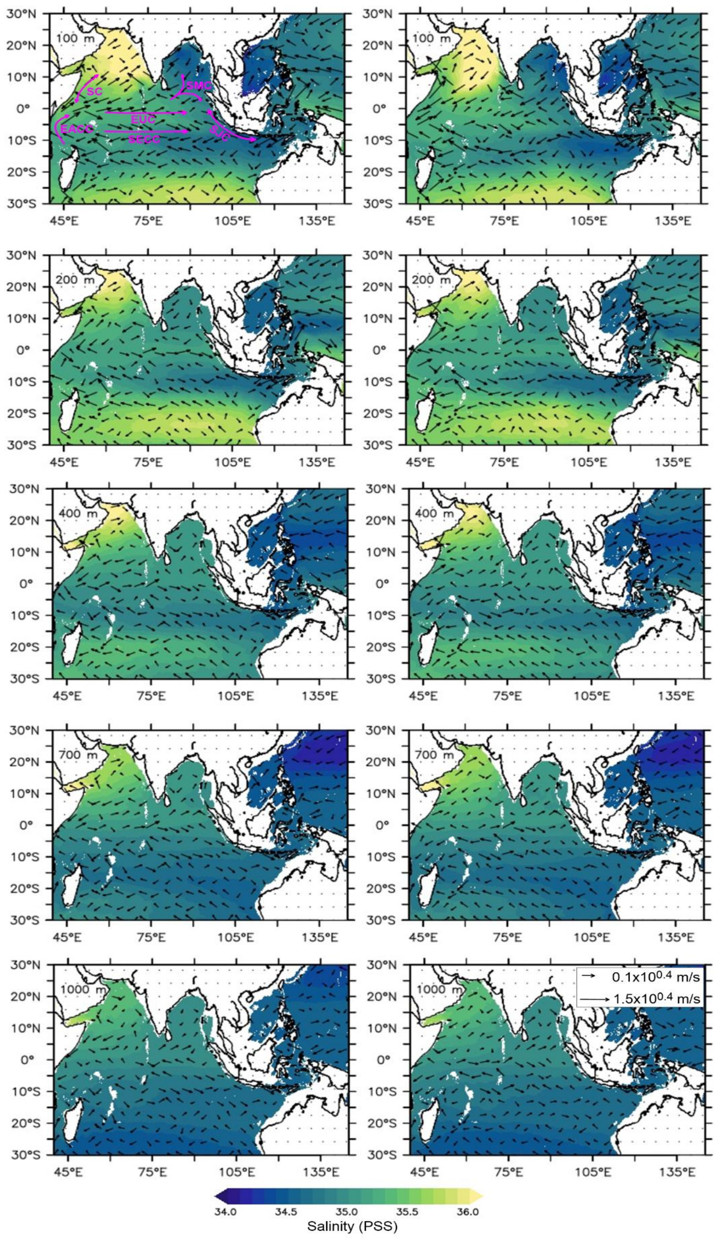

Figure 5. (Left) Salinity (color) and currents (arrows) in the Indian Ocean across depths at 100, 200, 400, 700 and 1,000 m the boreal winter (Jan-Mar). **(Right)** Similarly for the boreal summer (July-Sept). Equatorial ocean currents in the Indian Ocean are shown in the upper left panel: the Somali Current (SC), the East Africa Counter Current (EACC), the Equatorial Under Current (EUC), the South Equatorial Under Current (SEUC), and South Java Current (SJC). Salinity and currents data of CMEMS.

https://doi.org/10.5194/egusphere-2024-451
Preprint. Discussion started: 28 February 2024

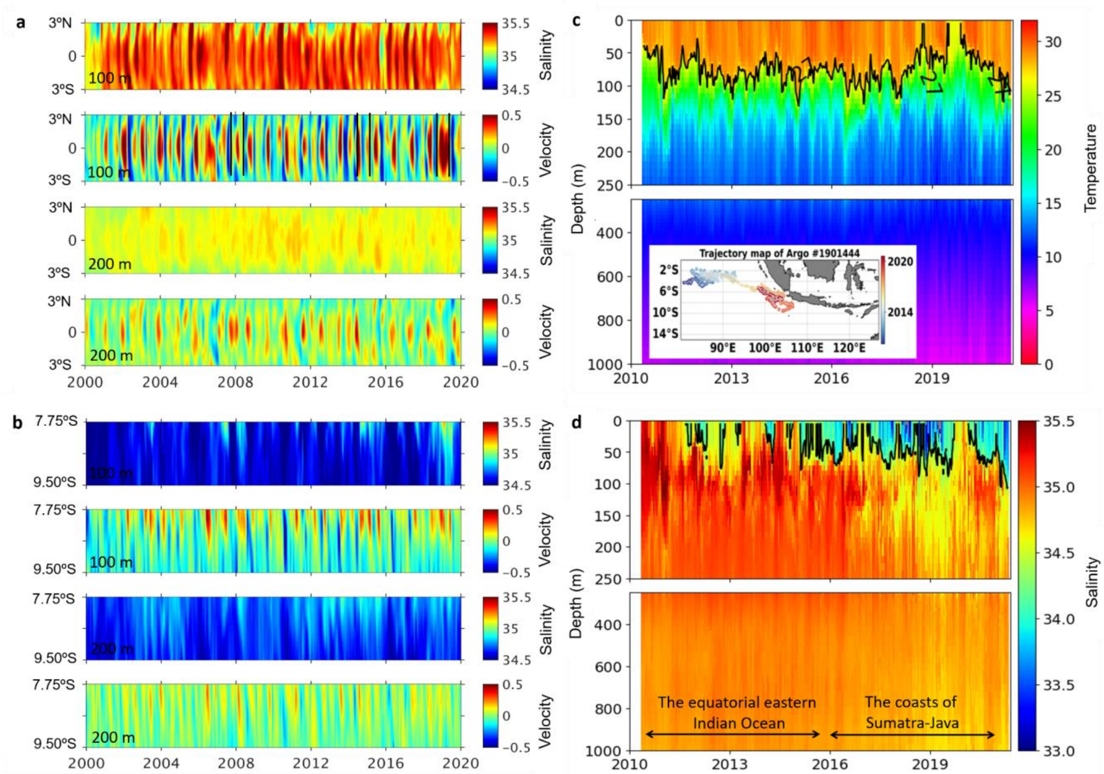

767

768 **Figure 6. (a)** Salinity (PSS) and velocity (m s^{-1}) in the equatorial Indian Ocean (3°N-3°S, 80.5°E) at
769 100 m and 200 m depths. **(b)** Similarly in southern Java (7.75-9.5°S, 107°E). Salinity and currents data
770 of CMEMS. **(c)** *In situ* temperature () from the Argo float ID #1901444 in the eastern Indian Ocean.
771 **(d)** Similarly for salinity.

https://doi.org/10.5194/egusphere-2024-451
Preprint. Discussion started: 28 February 2024

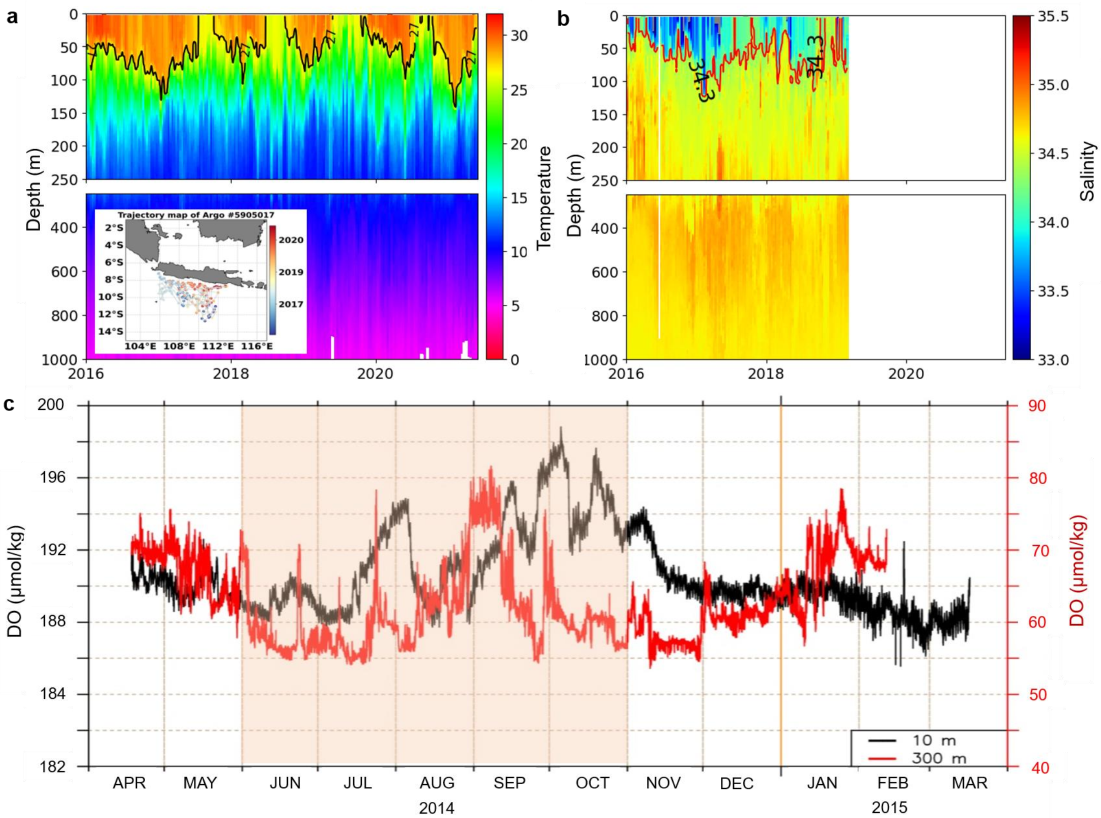

Figure 7. (a) *In situ* temperature in the southern Java from the Argo float ID #5905017. **(b)** Similarly for salinity. The black and red line mark the 27°C isotherm and 34.3 PSS isohaline, respectively. **(c)** DO measurements from a RAMA buoy in southern Java from April 2014 to March 2015 at 10 m (black) and 300 m (red) depths. Shaded in panel (c) denotes upwelling season.

https://doi.org/10.5194/egusphere-2024-451
Preprint. Discussion started: 28 February 2024

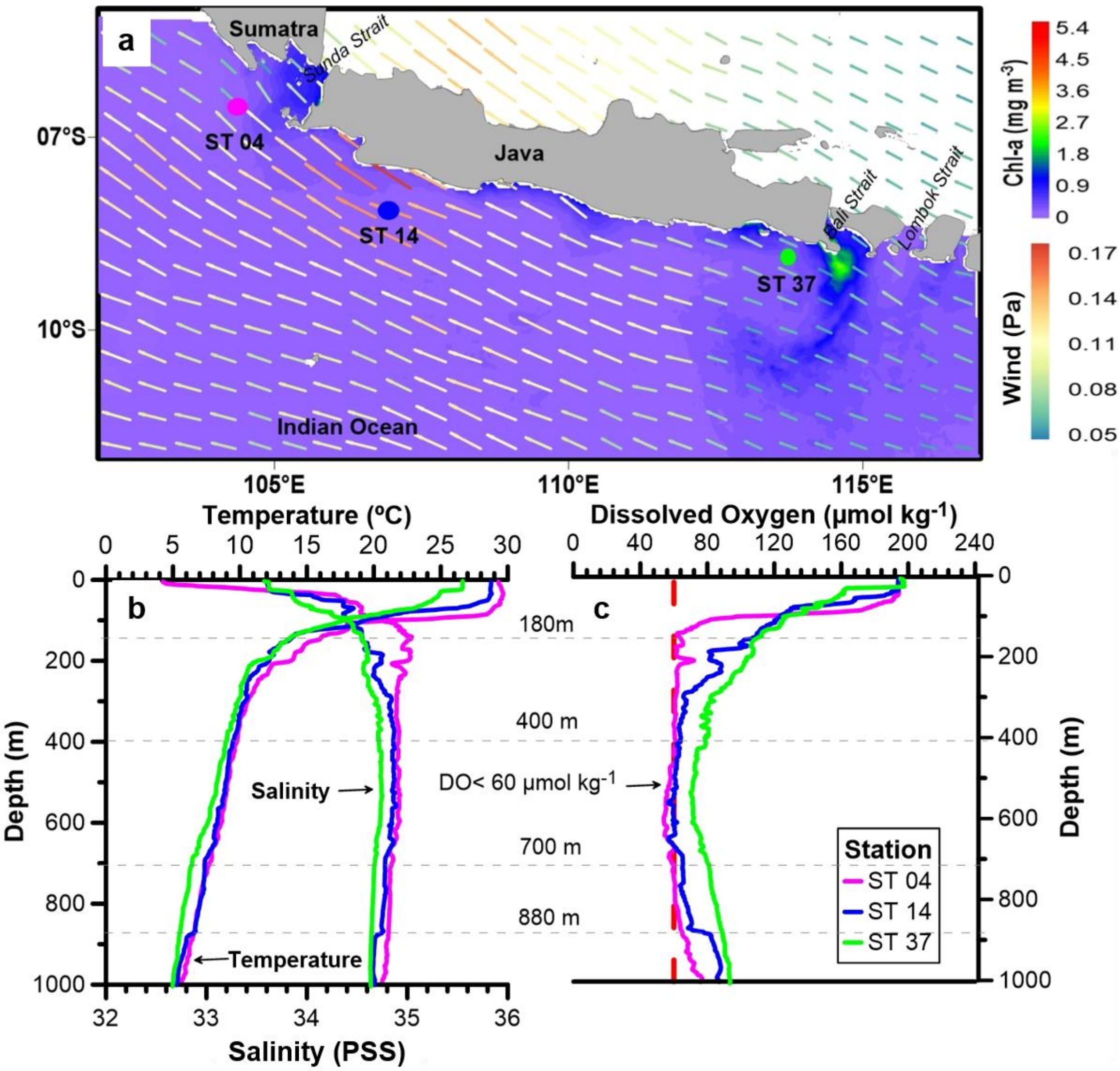

Figure 8. (a) Locations of observational stations 04, 14 and 37 in southern Java during the July 2022 cruise with mapped chlorophyll-a (colors) and westward wind stress (arrows). **(b)** Vertical profiles of temperature and salinity. **(c)** Vertical profile of DO. The chlorophyll-a and westward wind stress data of NOAA.

https://doi.org/10.5194/egusphere-2024-451
Preprint. Discussion started: 28 February 2024

782 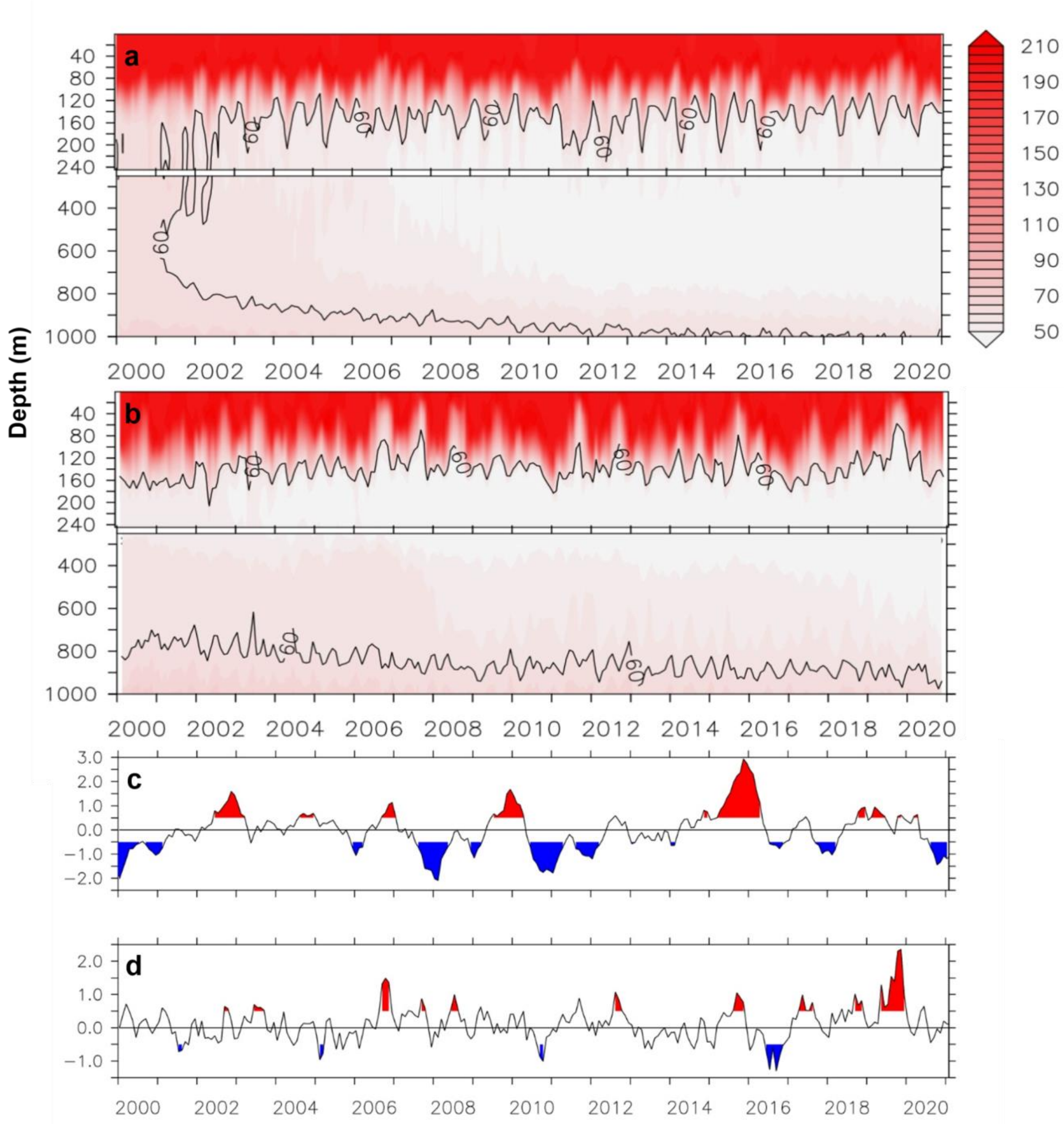

783 **Figure 9. (a)** Comparison of DO (μmol kg^{-1}) in western Sumatra (3°S, 98°E) between 2000-2020
784 against the IOD and ENSO shown in panels **c** and **d**, respectively. **(b)** Similarly in southwestern Java
785 (7.75ºS, 107ºE). Black lines mark the OLZ (DO=60 μmol kg^{-1}) thresholds. IOD and Niño 3.4 indices
786 apply the ± 0.5ºC thresholds.